Applications of brake pads on Asymmetrical Friction Connections (AFC)

J. Chanchí Golondrino

University of Canterbury, New Zealand - National University of Colombia, Colombia

G.A. MacRae, J.G. Chase, & G.W. Rodgers

University of Canterbury, New Zealand.

G.C. Clifton

University of Auckland, New Zealand.

2013 NZSEE Conference

ABSTRACT: This paper reports on the quasi-static testing of Asymmetrical Friction Connection specimens (AFC) using friction surfaces made of a non asbestos brake pad material termed D3923. Three brake pad configurations were considered: bonded over the total sliding surface, bonded on the vicinities of the bolt holes, and bonded on machined areas at the vicinities of the bolt holes. For each brake pad configuration the hysteretic behaviour of the connection is described. Results show that the hysteresis loop of the connection is almost square and becomes stable after the brake pad material has reached a steady wear state. For the steady wear state, effective friction coefficients of 0.16 were found regardless the brake pad configuration.

1 INTRODUCTION

Several experimental studies have shown the benefits in terms of friction coefficients and stable hysteretic behaviours of symmetrical friction connections equipped with brake pads as friction surface (Pall 1979, Tyler 1985, Kim 2004). Early applications of this technology used Asbestos based brake pads given their stable and low degradation hysteretic behaviour (Pall 1979). However, this material is not longer used to manufacture brake pads given the environmental and health implications (Chan 2004). For that reason, the use of non-asbestos materials to manufacture brake pads for friction applications has become popular. Recent applications of this type of brake pad material are those reported by Kim (2004) when successfully using NF-916 material as brake pad in symmetrical friction connections. In these studies it was shown that by bonding the brake pad material on recessed areas of the steel plates, the connection can dissipate energy in a stable and repeatable manner. To date, there is not reference of any experimental study applying the benefits of non-asbestos materials as an alternative friction surface to be applied on asymmetrical friction connections (AFC). This paper describes the application of a non-asbestos brake pad material termed D3923 (Ferotec Friction 2011) on AFC specimens and aims to answer these questions:

1. What is the hysteresis loop shape of AFC specimens using bonded brake pads of D3923 as friction surface?
2. Do AFC specimens using bonded brake pads of D3923 degrade during cyclic loading?
3. What are typical values of the effective friction coefficient of AFC specimens using brake pads of D3923?
4. What are benefits of using brake pads of D3923 bonded on recessed surfaces of AFC specimens?

2. MATERIALS

2.1 Asymmetrical Friction Connections (AFC)

Asymmetrical Friction Connections consist of three steel plates and two metallic or non-metallic plates termed shims. These five components are assembled by means of high strength bolts using Belleville springs (Figure 1a). The energy dissipation mechanism of this type of connection is based on forcing the slotted plate to slide across the connection arrangement (Figure 1b), and it can be used as an alternative to dissipate energy in steel framing systems (Figure 1c). Typical configurations are based on either placing the AFC detail in beam column joints where the slotted plate slides as result of the joint rotation (Clifton 2005), or within braces where the slotted plate slides as the brace axially deforms (MacRae 20009, Chanchi et al. 2012). Different material alternatives can be considered as shims; metallic options include aluminium, brass, bisalloy 400 and bissalloy 500 and consist of plates with thickness ranging between 3 and 6mm (Khoo et al. 2011, Chanchí et al. 2012). Non-metallic options are associated with the use of brake pads that are bonded to the steel plates and with similar thickness as those used in the case of metallic shims. One possible alternative to be considered in this category is the use of brake pads made of the composite friction material D3923 bonded onto the fixed plate and the cap plate (Figure 1a).

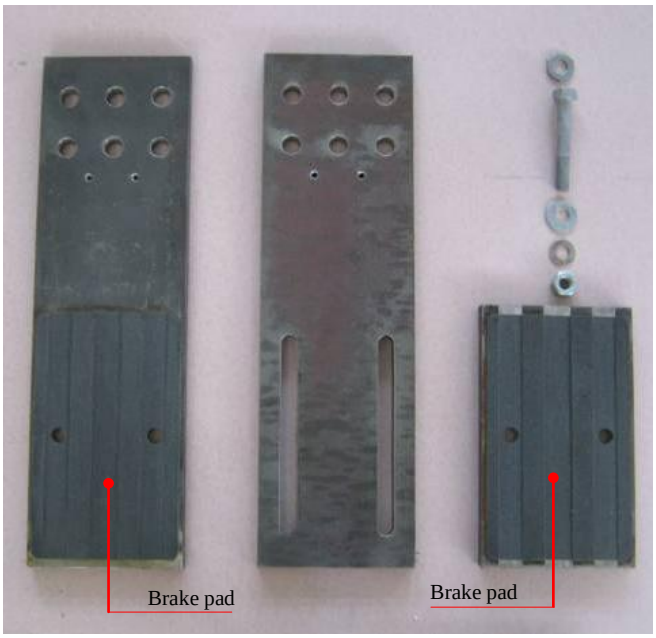

a. Fixed plate, slotted plate, cap plate, and bolt assembly

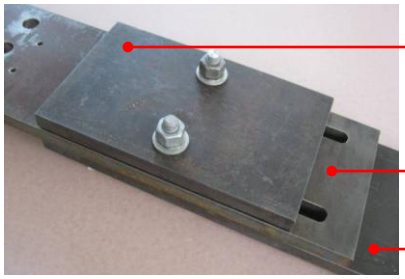

b. Plan view of AFC specimen

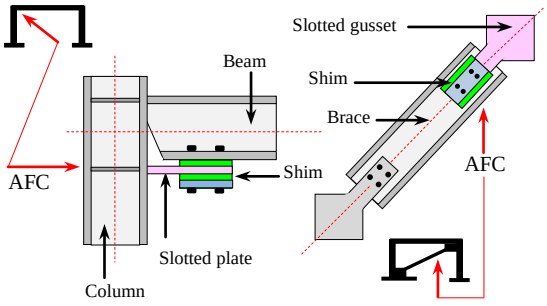

c. AFC configurations in steel framing systems

Figure 1. Components and Assembly of AFC specimens using D3923 brake pad material.

2. 2 Non Asbestos D3923

D3923 is a friction material that is manufactured and distributed by Ferotec Friction Inc. D3923 can be described as flexible non-asbestos moulded material used in the automotive industry to manufacture brake linings because its stability on friction coefficient and wear resistant properties. This material is manufactured from filler materials such as Vermiculite (mica), Barium sulphate and Calcium carbonate that are reinforced by the addition of glass and cellulose fibres (Ferotec Friction2011). Bonding of this material on steel surfaces require the use of Araldite based adhesives; in the bonding procedure surfaces are positioned together and subjected to temperatures of 150-200°C and clamping pressures of 0.35-1.0MPa (Huntsman 2004).

2.3 Brake pads configurations

Three brake pads configurations were considered as shims bonded on the surface of the fixed and end cap plates that are in direct contact with the central slotted plate. The first configuration was based on bonding the brake pad over the total contact surface (Figure 2a). In the second configuration the brake pad was bonded over the total surface and profiled in such as way that only strips at both sides of the holes were in contact with the sliding surfaces of the slotted plate (Figure 2b). The third configuration was assembled by bonding the brake pad on a recess of 1.5mm depth machined over the total contact surface and the brake pad was profiled in a similar way as that one used in the second configuration (Figure 2c). The second and third configurations were adapted from those configurations suggested by Kim 2004 when using NF916 non-asbestos organic material on bolted slotted connections. For whole configurations brake pads with thickness of 3.0 mm were used and they were bonded over the steel surfaces previously cleaned and degreased using the procedure described in section 2.2.

a. Bonded over all surface

b. Bonded over all surface and profiled to stripped surface finished

c. Bonded over recessed surface and profiled to stripped surface finished

Figure 2. Brake pad disposition on end cap of Asymmetrical Friction Connections

2.4 AFC specimens assembly

Two AFC specimens with slot lengths of 220mm were considered at each brake pad configuration. Specimens were assembled using 20mm thickness Grade 300 steel plates, and two M16 Grade 8.8 - 110 mm length galvanized bolts with single Belleville washer. Bolts were tensioned up to the proof load as recommended by NZS 3404 (2009) in the case of friction type connections. To achieve this proof load requirement during the connection assembling process, bolts were subjected to a torque values of 300N-m from the snug tighten condition. This torque value was defined from a torque – induced bolt elongation relationship developed by recording the elongation of three bolts assembled in similar AFC specimens and subjected to torque values increased from the snug tight condition up to the bolt failure (Figure 3a). In this relationship, the torque that develops the proof load condition was defined as the torque that induces an elongation similar to that exhibited by 3 bolts when reaching a force of 95kN in a tensile testing where the testing length was similar to the connection grip length (Figure 3b). It can be seen in Figure 3a that the proof load of bolts can be reached using torque values of 200-300N-m. The upper limit of this range was used given the variability on the torque –induced bolt elongation relationship; this variability is attributed to the surface finish of zinc galvanized bolts. In addition, assembling process of AFC specimens was also correlated with the part nut rotation method; in this case the proof load on bolts was reached at nut rotations measured from the snug tight condition of 1/4 -1/2turn.

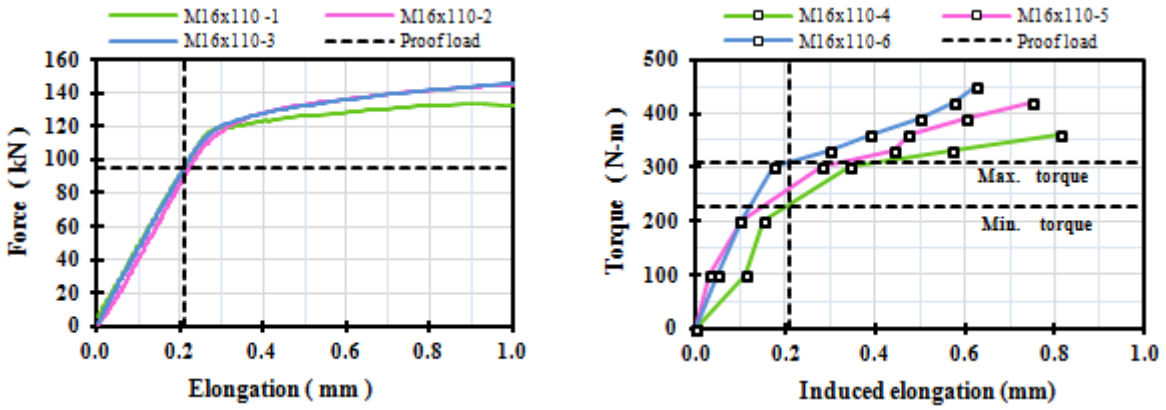

a. Axial force – elongation relationship recorded for bolts with grip lengths of 72mm

b. Torque – induced elongation relationship recorded from the snug tighten condition

Figure 3. Bolt assembling relationship

3. METHODS

3.2 Testing setup and displacement regime

Testing was carried out on a horizontal setup comprised of a fixed bracket attached to a reaction frame and a moving bracket attached to a shaking table. AFC specimens were connected to the fixed and moving brackets by means of 6 bolts M20 Grade 8.8 at each end. This setup was instrumented with a load cell located on the reaction frame and a potentiometer across the connection stroke (Figure 4a and 4b). The sliding mechanism was initiated by applying a displacement regime on the slotted plate connected to the shaking table.

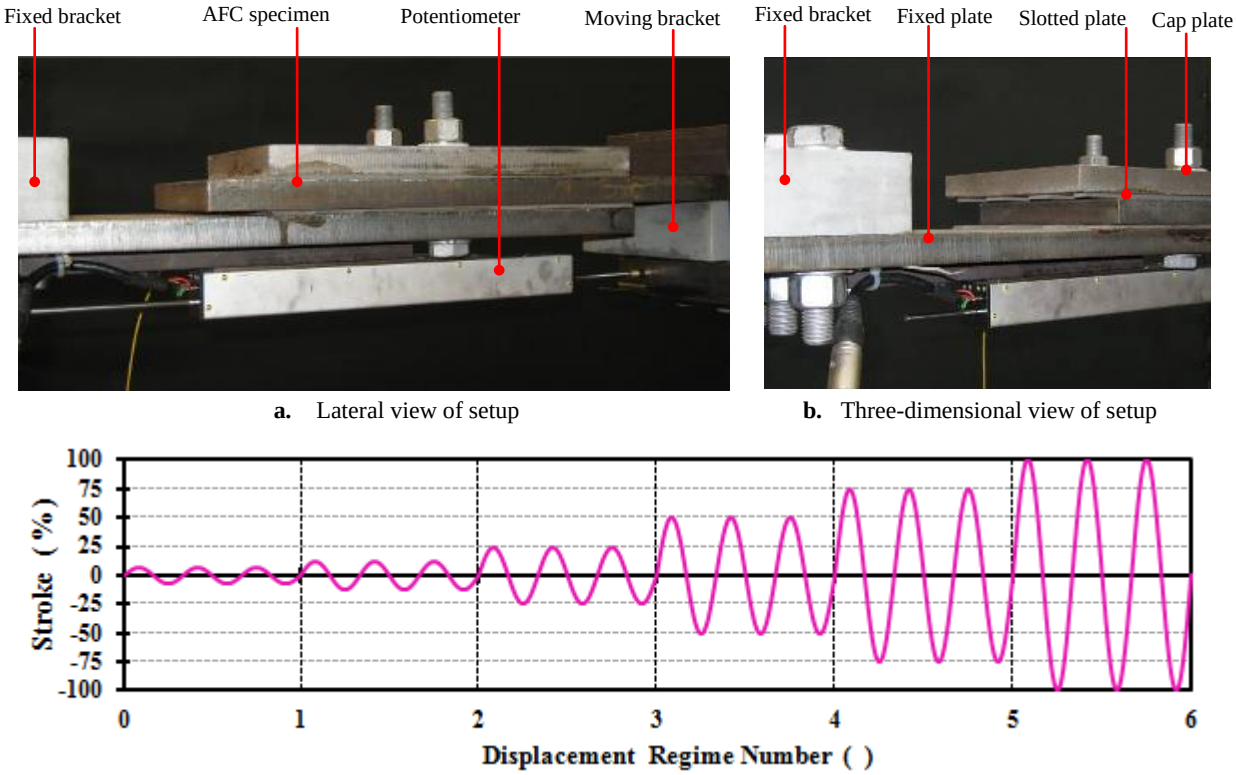

a. Lateral view of setup

b. Three-dimensional view of setup

c. Imposed displacement regime

Figure 4. Testing setup and imposed displacement regime

The displacement regime comprised 20 sinusoidal cycles with a maximum velocity of 15mm/s and amplitudes varying from 3.13 to 100% of the connection slot (Figure 4C). AFC specimens were subjected to two runs of the displacement regime; the second run was carried out after specimens return to room temperature after a cooling down period at room temperature conditions.

3 RESULTS AND ANALYSIS

3.1 Hysteresis Loop Shape

Hysteresis loop shapes for the three brake pad configurations were found to be almost rectangular and characterized by the development of increased forces at sliding distances less than 10mm. These increased forces were reduced gradually as the sliding distance was increased from 10 to 75mm, so that almost constant forces were developed when the specimen was sliding over the total sliding length. This reduction in force was more accentuated in brake pads bonded over all surfaces rather than in configurations where the brake pads were profiled at both sides of the bolt holes and it can attributed to the loss of bolt tension caused as the brake pad surfaces are worn by sliding action of the slotted plate (Figure 5). Brake pads were worn given the non-homogeneous distribution of the reinforcing fibres, for that reason at initial sliding stages the softer components of the brake pad material are removed until localized areas of wear resistant components of the brake pad are in direct contact with the steel surface (Eriksson et al. 2002). The stability and the magnitude of the sliding force were found to vary with the brake pad configuration. While specimens with brake pads configurations bonded on non-machined steel surfaces exhibited unstable hysteresis loops with larger sliding forces (Figure 5a and 5b); specimens using brake pads bonded on recessed steel surfaces developed lower sliding forces with an almost stable hysteresis loops. Thus, showing the benefit of confining the brake pad material not only in terms of hysteresis loop stability, but also because in this type of configuration undesirable brake pad movements are prevented (Kim 2004). The sliding mechanism of the three brake pad configurations was found to be similar and characterized by initial stiff segment where the specimen behaves elastic with no sliding (Segment a-b in Figure 5). After this elastic stage, a slight reduction in stiffness associated with the activation of the sliding mechanism at the interface slotted – fixed plate is presented (Segment b-c in Figure 5). This reduction in stiffness is followed by a final segment where the stiffness is similar as that one of the initial segment, and it is presented when bolts are in direct bearing with the fixed and cap plate allowing the onset of the activation of the full sliding mechanism (segment c-d in Figure 5).For whole configurations no degradation on the bonding material or fracture or the brake pads were noticed, in addition temperatures in the range 40 - 60°C were recorded at the external surface of the specimen after was subjected to the first run of the displacement regime.

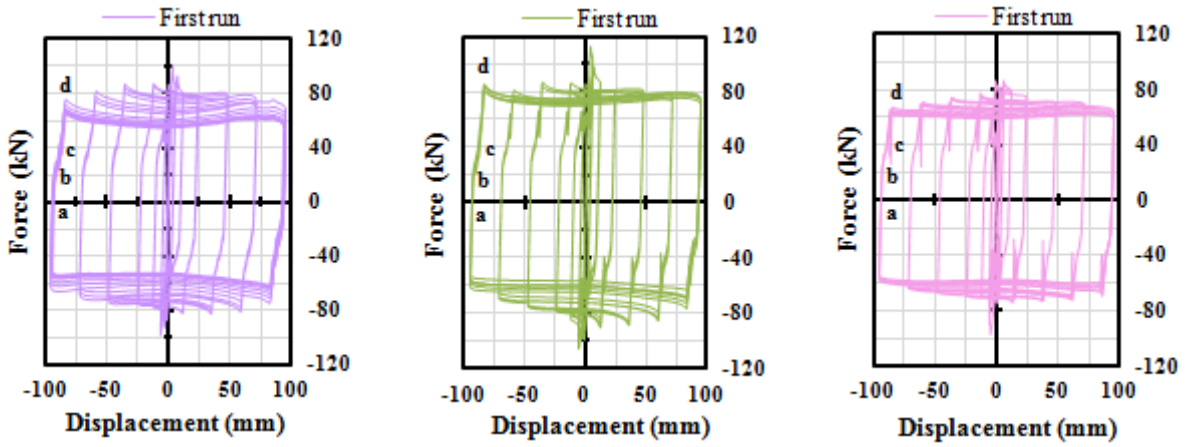

a. Bonded over all surface

b. Bonded over all surface and profiled to stripped surface finished

c. Bonded over recessed surface and profiled to stripped surface finished

Figure 5. Hysteresis loops of AFC specimens using three different brake pad configurations tested with one run of the displacement regime

3.2 Degradation

To describe the degradation of the three brake pad configurations, specimens were subjected to a second run of the displacement regime. This second displacement regime was run after each AFC specimen was cooled down at room temperature to remove any heating effects from the initial regime that could affect the behaviour of the brake pad material. In this second run an almost stable hysteretic behaviour was found for whole brake pads configurations; constant sliding forces were recorded over the total sliding length (Figure 6). When comparing the lowest sliding force level exhibited in the first regime run with the constant sliding force level developed in the second regime run for whole brake pad configurations, it can be seen that reductions of 17% were presented for configurations where the brake pads were bonded on non-machined steel surfaces (Figure 6a and 6b), and reductions of 5% for specimens using brake pads bonded on recessed steel surfaces (Figure 6c). In addition it can be also noted that in the second regime run the sliding force is approximately 60kN regardless of the brake pad configuration. Stability of the hysteresis loop is associated with the development of a steady wear state presented when the localized wear resistant materials of the brake pad carry the large proportion of the load; thus protecting the softer components of the brake pad such as filling materials (Eriksson et al. 2002).

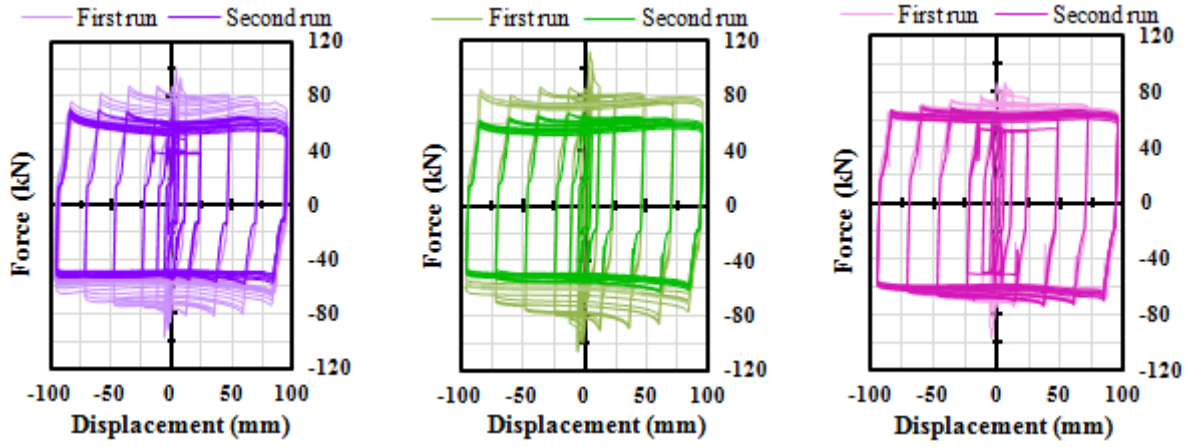

a. Bonded over all surface

b. Bonded over all surface and profiled to stripped surface finished

c. Bonded over recessed surface and profiled to stripped surface finished

Figure 6. Hysteresis loops of AFC specimens using three different brake pad configurations tested with two runs of the displacement regime

3.3 Effective friction coefficient

The effective friction coefficient defined as the force developed by the AFC specimen on both shear planes for each bolt divided by the installed bolt tension was calculated for the breakaway and sliding condition using Equation 1. In this equation, F is either the breakaway or sliding force, n is the number of bolts, η is the number of shear planes, and T is the proof load as defined in section 2.4.

$$\mu_{effective} = \frac{F}{n \times \eta \times T} \quad (1)$$

The breakaway condition was associated with the initial force-displacement curve exhibited by specimens before a steady sliding state was reached (Figure 7). Effective friction coefficients were found to vary in the range (0.20 - 0.24); the lower and upper limits of this range were associated to brake pad configurations bonded on non machined surfaces and on recessed surfaces respectively. For the sliding condition the constant sliding forces exhibited by specimens in the second regimen run

were considered; in this case the effective friction coefficient were found to be similar for whole brake pad configurations and near 0.16. In both cases values of effective friction coefficient are approximately half of those reported on the material data sheet of the composite material D3923 (Ferotec 2011). Reasons of this can be associated with the different load conditions that the material was exposed when assessing the friction coefficient. While the provider used a rotary loading system where the specimen is loaded by tangential forces (SAE J661, 1997); in AFC specimens friction is developed by forces parallel to the brake pad surfaces. In addition, effective friction coefficients calculated with Equation 1 are based on the nominal proof load of the bolts, so no loss in tension due to the brake pad degradation is considered. For that reason the effective friction coefficient for the breakaway condition should be considered when designing any application of AFC specimen using this type or material, or the adequate selection of an over strength factor to design the structure using this type of dissipater is recommended.

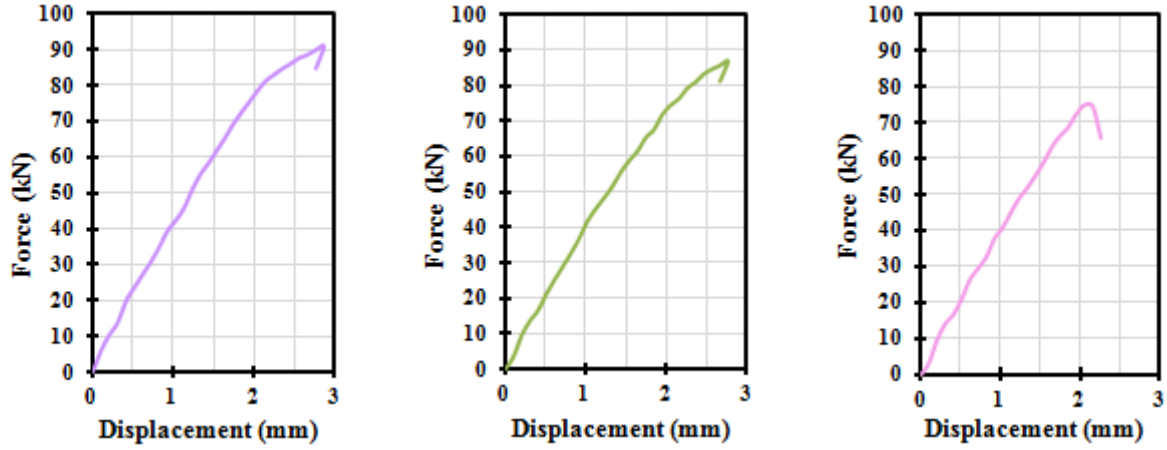

a. Bonded over all surface

b. Bonded over all surface and profiled to stripped surface finished

c. Bonded over recessed surface and profiled to stripped surface finished

Figure 7. Breakaway curve of AFC specimen using three different brake pad configurations

4 CONCLUSIONS

This paper describes the behaviour of Asymmetrical Friction Connections using three different configurations of brake pads made of the composite material D3923; it was shown that:

1. Hysteresis loop of AFC specimens using brake pads made of D3923 is almost rectangular. Increased forces up to 40% were observed at initial sliding cycles, this increased forces reduce as the brake pad material reach a steady wear state.
2. Sliding forces of tested brake pad configurations exhibited degradations of 5-17%; these degradations are attributed to the loss of bolt tension presented when the brake pad surfaces are worn during the sliding action of the slotted plate.
3. By using brake pads made of D3923 bonded on recessed surfaces of AFC specimens, more stable hysteresis loop were obtained and degradations on the sliding force were reduced up to 5%.
4. The effective friction coefficient of AFC specimens using brake pads made of D3923 was found to vary in the range 0.20 -0.24 for the breakaway condition, and values of 0.16 were found for the sliding condition.

5 REFERENCES

Chan, D. & Stachowiak, G.W. (2004). Review of automotive brake friction materials. *Journal of Automobile Engineering.* Vol. 218, 253-266.

Chanchí, J.C., MacRae, G.A., Chase, J.G., Rodgers, G.W., Clifton, G.C, & Munoz, A. (2012). Design considerations for braced frames with asymmetrical friction connections (AFC). *STESSA 2012, Santiago de Chile*, January.

Chanchí, J.C., MacRae, G.A., Chase, J.G., Rodgers, G.W., & Clifton, G.C. (2012). Behaviour of asymmetrical friction connections using different shim materials. *Proceedings of the New Zealand Society of Earthquake Engineering- Annual Conference. Christchurch* - New Zealand.

Clifton, G.C. (2005). Semi-Rigid Joints for Moments Resisting Steel Framed Seismic Resisting Systems. *Published PhD Thesis, Department of Civil and Environmental Engineering.* University of Auckland – New Zealand.

Erikson, M., Bergman, F., & Jacobson, S. (2002). On the nature of tribological contact in automotive brakes. *International Journal on the Science and Technology of Friction, Lubrication and Wear*. Vol. 252, 26-36.

Ferotec Friction, Inc. (2011). Product Data Sheet – Friction Material Composite D3923.

Ferotec Friction, Inc. (2011). Material Safety Data Sheet – Friction Material Composite D3923/ D3924.

Khoo, H.H., Clifton, C., Butterworth, J., MacRae, G. and Ferguson, G. (2011) Influence of steel shim hardness on the Sliding Hinge Joint. Journal of Constructional Steel Research.

Huntsman Structural Adhesives. (2004). Brake and Cluth Bonding, Araldite 71 brake and bonding ashesive.

Kim, H.J. (2004). Experimental Characterization of Bolt Stressed Non- Asbestos Organic (NAO) Material-to-Steel-Interfaces. Un*published PhD Thesis, Department of Civil and Environmental Engineering.* University of Toronto – Canada.

MacRae, G. A. (2008). A New Look at Some Earthquake Engineering Concepts. M. J. *Nigel Priestley Symposium* Proceedings, IUSS Press, 2008.

Pall, A.S. (1979). Limited Slip Bolted Joints – A Device to Control the Seismic Response of Large Panel Structures. *Unpublished PhD Thesis, Faculty of Engineering*. Concordia University – Canada.

The International Society for Advancing Mobility Land Sea and Space – SAE. (1997). Brake lining quality test procedure (SAEJ661).

Standards New Zealand. (2009). NZS 3404: Part 1: 2009 – Steel Structures Standard. Wellington – New Zealand.

Tyler, R.G. (1985). Test on Brake Lining Damper for Structures. *Bulletin of the New Zealand Society for Earthquake Engineering.* 18 (3), pp 280-284.